*Quantum Electronics* **36** (12) 1161 – 1167 (2006) 

*DYNAMIC PROCESSES IN LASERS*

PACS numbers: 42.55.Rz; 42.60.Mi; 42.65.Ky; 42.65.Sf
DOI: 10.1070/QE2006v036n12ABEH013375

# Simulation of the dynamics of a multimode bipolarisation class B laser with intracavity frequency doubling

P.A. Khandokhin

***Abstract*. A model of a multimode bipolarisation solid-state laser with intracavity frequency doubling is developed. The interaction of different longitudinal modes is described within the framework of rate-equation approximation while the interaction of each pair of orthogonally polarised modes with identical longitudinal indices is described taking into account the phase-sensitive interaction of these modes. Comparison with the experimental data is performed.**

***Keywords***: *relaxation oscillations, spatial population-inversion gratings, angular burning out of population inversion, nonlinear frequency conversion, Hopf bifurcation, instability*.

## 1. Introduction

It has been found in experimental studies of the polarisation dynamics of solid-state lasers (including fibre lasers) that the spectra of intensity fluctuations of each polarisation mode of bipolarisation lasers (both multimode [1 – 4] and single longitudinal-mode lasers [5, 6]) contain several resonance peaks. These peaks point to the existence of several types of relaxation oscillations: high frequency oscillations caused by in-phase oscillations in all the modes and one or two types of polarisation oscillations caused by competitive interaction of orthogonally polarised modes. These types of relaxation oscillations have been observed in each polarisation mode which is understood as an ensemble of all longitudinal modes with the same polarisation. These specific features of low-frequency polarisation dynamics are well described by the model of longitudinally single-mode bipolarisation lasers, which takes into account the phase-sensitive interaction of orthogonally polarised modes [2, 5]. Although the simplest model of a bipolarisation laser qualitatively agrees with the experimental results, the question of how other longitudinal modes in the selected polarisation mode, which are involved in lasing, can be represented in the low-frequency dynamics, requires an answer.

**P.A. Khandokhin** Institute of Applied Physics, Russian Academy of Sciences, ul. Ul'yanova 46, 603950 Nizhnii Novgorod, Russia; e-mail: khando@appl.sci-nnov.ru

Received 23 August 2006
*Kvantovaya Elektronika* **36** (12) 1161 – 1167 (2006)
Translated by I.A. Ulitkin

It was pointed out in [4] that involvement of a new mode in lasing can be accompanied by the appearance of a resonance peak in the spectrum of intensity fluctuations of a separate polarisation mode. To answer the above question, we developed a model of a bipolarisation class B laser in which each polarisation mode consists of an arbitrary number of longitudinal modes. In this case, it is quite natural to describe the interaction of modes with different longitudinal indices within the framework of rate-equation approximation [7, 8]. At the same time, the interaction of orthogonally polarised modes with the same longitudinal spatial structure (with equal longitudinal indices) will be described using the approach [5], which takes into account the phase-sensitive interaction of these modes.

The experimental results of Ref. [4] in which the features of the optical spectrum of a bipolarisation laser were observed, served as an additional impetus to the development of a model of a multimode bipolarisation laser. Along with the 'rarefaction' of the optical spectrum caused by the inhomogeneous gain distribution along the resonator axis, the generation of orthogonally polarised modes at different longitudinal modes was observed in this paper. The proposed model taking into account partial filling of the laser cavity with the active medium [7, 8] allows one to explain this peculiarity of the lasing spectrum of orthogonally polarised modes.

## 2. Model of a multimode bipolarisation laser

When deriving equations describing the dynamics of a multimode laser, it is necessary to expand the laser field in the cavity modes. We will take into account the fact that the field of each longitudinal mode consists of two orthogonally polarised components:

$$\boldsymbol{E}_j = (E_j^x \boldsymbol{U}_j^x + E_j^y \boldsymbol{U}_j^y) \exp(\mathrm{i}\omega_j t) + \text{c.c.}, \tag{1}$$

where $E_j^{x,y}$ are slowly varying field amplitudes with orthogonal polarisations of the $j$th longitudinal mode; $\omega_j$ is the optical frequency of this mode. The eigenmodes have the form

$$\boldsymbol{U}_j^{(m)} = \sqrt{2}\boldsymbol{e}_m^0 \cos k_j z, \quad m = x, y, \tag{2}$$

where $k_j$ is the wave number of the $j$th longitudinal mode. In the general case, eigenpolarisations are elliptical, therefore, expressions for their unit vectors $\boldsymbol{e}_m^0$ can be written in the form:

$$\boldsymbol{e}_x^0 = \boldsymbol{x}^0 \cos\vartheta + \mathrm{i}\boldsymbol{y}^0 \sin\vartheta, \tag{3}$$

$$\boldsymbol{e}_y^0 = \mathrm{i}\boldsymbol{x}^0 \sin\vartheta + \boldsymbol{y}^0 \cos\vartheta, \tag{4}$$

where $\boldsymbol{x}^0$ and $\boldsymbol{y}^0$ are Cartesian unit vectors coinciding with the orientation of principal axes of ellipses of the cavity eigenpolarisations; and the parameter $\vartheta$ determines the degree $\varepsilon_{1,2}$ of ellipticity of polarisation modes:

$$\varepsilon_{1,2} = |\tan\vartheta|^2. \tag{5}$$

We will assume that $K$ longitudinal modes can be involved in lasing. Then the laser field can be represented in the form:

$$\boldsymbol{E} = \sum_{j=1}^{K} \boldsymbol{E}_j\,. \tag{6}$$

We will describe the orientation of active dipoles within the assumptions made earlier in [5, 7, 8] taking the following into account. In crystals, active ions occupy certain positions inside the elementary cell of the crystal lattice. In the Nd : YAG crystal, there exist three such equally probable positions (in the centre of each of three mutually orthogonal faces of a cubic elementary cell [9]). In addition, in each of these positions neodymium ions can be oriented with equal probability along two orthogonal symmetry axes coinciding with the face diagonals. In this connection, we can expect that dipole moments of active ions will be oriented near several (in the general case, up to six) selected directions in space, preserving on the whole isotropic properties of the crystal. Therefore, we assume for simplicity that all active dipoles are linearly polarised and are randomly distributed in the plane perpendicular to the laser axis. Then,

$$\boldsymbol{d}_{\mathrm{a,e}}^0 = \frac{\boldsymbol{d}_{\mathrm{a,e}}}{|\boldsymbol{d}_{\mathrm{a,e}}|} = \boldsymbol{x}^0 \cos\Psi + \boldsymbol{y}^0 \sin\Psi, \tag{7}$$

where $\boldsymbol{d}_{\mathrm{a}}$ and $\boldsymbol{d}_{\mathrm{e}}$ are the dipole moments of absorption and emission transitions, respectively; the angle $\Psi$ varies from 0 to $\pi$. The linearly polarised pumping introduces additional corrections to the homogeneous angular (orientation) distribution of active dipoles of the absorption transition $f_{\mathrm{or}}^0(\Psi) = 1/\pi$ [3, 10, 11], which leads to the angular dependence of the pump parameter $A$ (the ratio of unsaturated population inversion to its threshold value) [5]:

$$A = A_0 \Phi_{\mathrm{or}}(\Psi), \tag{8}$$

where

$$\Phi_{\mathrm{or}} = \frac{a + b\cos^2(\Psi - \Psi_{\mathrm{pump}})}{1 + b\cos^2(\Psi - \Psi_{\mathrm{pump}})} \frac{1}{\Phi_{\mathrm{or}}^0},$$
$$\Phi_{\mathrm{or}}^0 = \frac{1}{\pi}\int_0^{\pi} \frac{a + b\cos^2(\Psi - \Psi_{\mathrm{pump}})}{1 + b\cos^2(\Psi - \Psi_{\mathrm{pump}})}\mathrm{d}\Psi = 1 - \frac{1-a}{\sqrt{1+b}}; \tag{9}$$

$\Psi_{\mathrm{pump}}$ is the angle between the $x$ axis and the pump electric field vector (upon longitudinal pumping). Parameters $a$ and $b$ determine the gain anisotropy, the parameter $a$ introduced phenomenologically in (9) corresponding to the condition $a \ll b$. These parameters are proportional to the pump power. For low pump powers, the parameter $b$ is small and the gain anisotropy is maximal. An increase in this parameter leads to a decrease in the effect of induced anisotropy, and within the limit of high pump powers (as was mentioned in [11]) the active medium becomes isotropic.

In addition to the angular inhomogeneity of active centre distribution $\Phi_{\mathrm{or}}(\Psi)$, under real conditions spatial inhomogeneity of their distribution along the resonator axis $\Phi_{\mathrm{sp}}(z)$ also takes place, which we will take into account by deriving equations in the form [7, 8]:

$$\Phi_{\mathrm{sp}}(z) = \begin{cases} \alpha L \exp(-\alpha z)/[1 - \exp(-\alpha l)], & 0 \leqslant z \leqslant l, \\ 0, & l < z \leqslant L, \end{cases} \tag{10}$$

where $\alpha$ is the pump-absorption coefficient; $L$ is the resonator length; and $l$ is the crystal length. Expression (10) takes into account the exponential pump decay ($\alpha \neq 0$) along the crystal filling partially the laser cavity, which corresponds to real experimental conditions.

Therefore, the interaction of bipolarisation laser field (6) with the linearly polarised dipoles, which have the azimuthal distribution $\Phi_{\mathrm{or}}(\Psi)$ (9) and the longitudinal spatial distribution $\Phi_{\mathrm{sp}}(z)$ (10) is described by a system of equations [5, 7, 8]

$$\frac{\mathrm{d}E_k^x}{\mathrm{d}\tau} = \frac{G}{2}\left\{(\mathrm{i}\delta_{\mathrm{f}} - 1)E_k^x + \frac{g_k}{L\pi}\int_0^{\pi}\int_0^{L} \Phi_{\mathrm{sp}}(z) D(z,\Psi)(\boldsymbol{d}_{\mathrm{e}}^0 \boldsymbol{U}_k^{x*}) \right.$$
$$\left. \times \left[E_k^x(\boldsymbol{d}_{\mathrm{e}}^{0*}\boldsymbol{U}_k^x) + E_k^y(\boldsymbol{d}_{\mathrm{e}}^{0*}\boldsymbol{U}_k^y)\right]\mathrm{d}z\mathrm{d}\Psi\right\},$$
$$\frac{\mathrm{d}E_k^y}{\mathrm{d}\tau} = \frac{G}{2}\left\{(-\mathrm{i}\delta_{\mathrm{f}} - 1)E_k^y + \frac{g_k}{L\pi}\int_0^{\pi}\int_0^{L} \Phi_{\mathrm{sp}}(z) D(z,\Psi)\right. \tag{11}$$
$$\left. \times (\boldsymbol{d}_{\mathrm{e}}^0 \boldsymbol{U}_k^{y*}) \left[E_k^x(\boldsymbol{d}_{\mathrm{e}}^{0*}\boldsymbol{U}_k^x) + E_k^y(\boldsymbol{d}_{\mathrm{e}}^{0*}\boldsymbol{U}_k^y)\right]\mathrm{d}z\mathrm{d}\Psi\right\},$$
$$\frac{\partial D}{\partial \tau} = A_0 \Phi_{\mathrm{or}}(\Psi) - D\left[1 + \sum_{j=1}^{K} g_j |E_j^x(\boldsymbol{d}_{\mathrm{e}}^{0*}\boldsymbol{U}_j^x) + E_j^y(\boldsymbol{d}_{\mathrm{e}}^{0*}\boldsymbol{U}_j^y)|^2\right],$$

where

$$g_j = \{1 + [(r-j)\Delta - \Delta_0]^2\}^{-1}, \quad j = 1, \ldots, K; \tag{12}$$

$r$ is the number of the mode closest to the gain line centre; $D$ is the population inversion; $G = 2\kappa/\gamma_{\parallel}$; $\tau = t\gamma_{\parallel}$; $2\delta_{\mathrm{f}} = (\omega_k^x - \omega_k^y)/\gamma_{\parallel}$ is the phase anisotropy of the cavity; $\omega_k^{x,y}$ are the eigenfrequencies of orthogonally polarised modes of the cavity; $\gamma_{\parallel}$ and $\kappa$ are the relaxation rates of the population inversion and the field in the cavity, respectively; $\Delta = (\omega_{k+1}^x - \omega_k^x)/\gamma_{\perp} = (\omega_{k+1}^y - \omega_k^y)/\gamma_{\perp}$ is the intermode interval normalised to the half-width of the homogeneous gain line $\gamma_{\perp}$; $\Delta_0 = (\omega_0 - \omega_r)/\gamma_{\perp}$; $\omega_0$ is the gain line centre; and $\omega_r = (\omega_r^x + \omega_r^y)/2$ is the frequency of the longitudinal mode closest to the gain line centre. In the system of equations (11), the interaction of different longitudinal modes remains within the framework of rate-equation approximation, while the interaction of orthogonally polarised modes with the same spatial structure is phase sensitive to the fields of these modes.

The interaction of elliptically polarised radiation with the ensemble of randomly oriented dipoles of the laser

transition leads to the azimuthal inhomogeneous distribution of population inversion (the effect of angular burning out of inversion):

$$D = D^0 + 2D^{\mathrm{c}}\cos 2\Psi + 2D^{\mathrm{s}}\sin 2\Psi + \dots . \tag{13}$$

In calculations of each angular harmonic $D^{(i)}$ ($i = 0$, c, s) of this distribution we retain only the spatially homogeneous component and first spatial harmonics (we neglect the highest spatial harmonics):

$$D^{(i)} = D_0^{(i)} + 2\sum_{j=1}^{K} D_j^{(i)}\cos\frac{2\pi q_j z}{L} + \dots , \tag{14}$$

where $q_j$ is the number of half-waves of the $j$th mode fit on the resonator length. As a result we obtain a system of $7K + 3$ equations (in real variables):

$$\begin{aligned}
\frac{\mathrm{d}E_k^x}{\mathrm{d}\tau} &= \frac{G}{2}\Bigg\{\Bigg(\mathrm{i}\delta_{\mathrm{f}} + g_k\Bigg[D_0^0 + D_0^{\mathrm{c}}\cos 2\vartheta \\
&+ \sum_{j=1}^{K}\Phi^{\mathrm{sp}}_{|k-j|}\left(D_j^0 + D_j^{\mathrm{c}}\cos 2\vartheta\right)\Bigg] - \varepsilon\sum_{j=1}^{K} g_j|E_j^y|^2 - 1\Bigg)E_k^x \\
&+ g_k\left[D_0^{\mathrm{s}} + \mathrm{i}D_0^{\mathrm{c}}\sin 2\vartheta + \sum_{j=1}^{K}\Phi^{\mathrm{sp}}_{|k-j|}\left(D_j^{\mathrm{s}} + \mathrm{i}D_j^{\mathrm{c}}\sin 2\vartheta\right)\right]E_k^y\Bigg\}, \\
\frac{\mathrm{d}E_k^y}{\mathrm{d}\tau} &= \frac{G}{2}\Bigg\{\Bigg(-\mathrm{i}\delta_{\mathrm{f}} + g_k\Bigg[D_0^0 - D_0^{\mathrm{c}}\cos 2\vartheta \\
&+ \sum_{j=1}^{K}\Phi^{\mathrm{sp}}_{|k-j|}\left(D_j^0 - D_j^{\mathrm{c}}\cos 2\vartheta\right)\Bigg] - \varepsilon\sum_{j=1}^{K} g_j|E_j^x|^2 - 1\Bigg)E_k^y \\
&+ g_k\left[D_0^{\mathrm{s}} - \mathrm{i}D_0^{\mathrm{c}}\sin 2\vartheta + \sum_{j=1}^{K}\Phi^{\mathrm{sp}}_{|k-j|}\left(D_j^{\mathrm{s}} - \mathrm{i}D_j^{\mathrm{c}}\sin 2\vartheta\right)\right]E_k^x\Bigg\},
\end{aligned} \tag{15}$$

$$\begin{aligned}
\frac{\mathrm{d}D_0^0}{\mathrm{d}\tau} &= A_0 - D_0^0 - \sum_{j=1}^{K}(D_0^0 + D_j^0)g_j\left(|E_j^x|^2 + |E_j^y|^2\right) \\
&- \sum_{j=1}^{K} g_j\Bigg\{\left(D_0^{\mathrm{c}} + D_j^{\mathrm{c}}\right)\left[\left(|E_j^x|^2 - |E_j^y|^2\right)\cos 2\vartheta + \mathrm{i}\left(E_j^{x*}E_j^y\right.\right. \\
&\left.\left. - E_j^x E_j^{y*}\right)\sin 2\vartheta\right] - \left(D_0^{\mathrm{s}} + D_j^{\mathrm{s}}\right)\left(E_j^{x*}E_j^y + E_j^x E_j^{y*}\right)\Bigg\}, \\
\frac{\mathrm{d}D_k^0}{\mathrm{d}\tau} &= -D_k^0 - \sum_{j=1}^{K}\left(\frac{1}{2}D_0^0 + D_j^0\right)g_j\left(|E_j^x|^2 + |E_j^y|^2\right) \\
&- \sum_{j=1}^{K} g_j\Bigg\{\left(\frac{1}{2}D_0^{\mathrm{c}} + D_j^{\mathrm{c}}\right)\left[\left(|E_j^x|^2 - |E_j^y|^2\right)\cos 2\vartheta + \mathrm{i}\left(E_j^{x*}E_j^y\right.\right. \\
&\left.\left. - E_j^x E_j^{y*}\right)\sin 2\vartheta\right] - \left(\frac{1}{2}D_0^{\mathrm{s}} + D_j^{\mathrm{s}}\right)\left(E_j^{x*}E_j^y + E_j^x E_j^{y*}\right)\Bigg\}, \\
\frac{\mathrm{d}D_0^{\mathrm{c}}}{\mathrm{d}\tau} &= A^{\mathrm{c}} - D_0^{\mathrm{c}} - \sum_{j=1}^{K}(D_0^{\mathrm{c}} + D_j^{\mathrm{c}})g_j\left(|E_j^x|^2 + |E_j^y|^2\right) \\
&- \frac{1}{2}\sum_{j=1}^{K}\left(D_0^0 + D_j^0\right)g_j\Bigg[\left(|E_j^x|^2 - |E_j^y|^2\right)\cos 2\vartheta + \mathrm{i}\left(E_j^{x*}E_j^y\right. \\
&\left. - E_j^x E_j^{y*}\right)\sin 2\vartheta\Bigg], \\
\frac{\mathrm{d}D_k^{\mathrm{c}}}{\mathrm{d}\tau} &= -D_k^{\mathrm{c}} - \sum_{j=1}^{K}\left(\frac{1}{2}D_0^{\mathrm{c}} + D_j^{\mathrm{c}}\right)g_j\left(|E_j^x|^2 + |E_j^y|^2\right) \\
&- \frac{1}{2}\sum_{j=1}^{K}\left(\frac{1}{2}D_0^0 + D_j^0\right)g_j\Bigg[\left(|E_j^x|^2 - |E_j^y|^2\right)\cos 2\vartheta + \mathrm{i}\left(E_j^{x*}E_j^y\right. \\
&\left. - E_j^x E_j^{y*}\right)\sin 2\vartheta\Bigg], \\
\frac{\mathrm{d}D_0^{\mathrm{s}}}{\mathrm{d}\tau} &= A^{\mathrm{s}} - D_0^{\mathrm{s}} - \sum_{j=1}^{K}(D_0^{\mathrm{s}} + D_j^{\mathrm{s}})g_j\left(|E_j^x|^2 + |E_j^y|^2\right) \\
&- \frac{1}{2}\sum_{j=1}^{K}\left(D_0^0 + D_j^0\right)g_j\left(E_j^{x*}E_j^y + E_j^x E_j^{y*}\right), \\
\frac{\mathrm{d}D_k^{\mathrm{s}}}{\mathrm{d}\tau} &= -D_k^{\mathrm{s}} - \sum_{j=1}^{K}\left(\frac{1}{2}D_0^{\mathrm{s}} + D_j^{\mathrm{s}}\right)g_j\left(|E_j^x|^2 + |E_j^y|^2\right) \\
&- \frac{1}{2}\sum_{j=1}^{K}\left(\frac{1}{2}D_0^0 + D_j^0\right)g_j\left(E_j^{x*}E_j^y + E_j^x E_j^{y*}\right).
\end{aligned} \tag{15}$$

The angular and spatial harmonics have the form:

$$\begin{aligned}
D_0^0(\tau) &= \frac{1}{\pi L}\int_0^L\int_0^\pi D(z,\Psi,\tau)\mathrm{d}z\mathrm{d}\Psi, \\
D_k^0(\tau) &= \frac{1}{\pi L}\int_0^L\int_0^\pi D(z,\Psi,\tau)\cos\frac{2\pi q_k z}{L}\mathrm{d}z\mathrm{d}\Psi, \\
D_0^{\mathrm{c}}(\tau) &= \frac{1}{\pi L}\int_0^L\int_0^\pi D(z,\Psi,\tau)\cos 2\Psi\,\mathrm{d}z\mathrm{d}\Psi, \\
D_k^{\mathrm{c}}(\tau) &= \frac{1}{\pi L}\int_0^L\int_0^\pi D(z,\Psi,\tau)\cos\frac{2\pi q_k z}{L}\cos 2\Psi\,\mathrm{d}z\mathrm{d}\Psi, \\
D_0^{\mathrm{s}}(\tau) &= \frac{1}{\pi L}\int_0^L\int_0^\pi D(z,\Psi,\tau)\sin 2\Psi\,\mathrm{d}z\mathrm{d}\Psi, \\
D_k^{\mathrm{s}}(\tau) &= \frac{1}{\pi L}\int_0^L\int_0^\pi D(z,\Psi,\tau)\cos\frac{2\pi q_k z}{L}\sin 2\Psi\,\mathrm{d}z\mathrm{d}\Psi.
\end{aligned}$$

The expansion coefficients $\Phi^{\mathrm{sp}}_{|k-j|}$ and angular harmonics $A^{\mathrm{c}}$, $A^{\mathrm{s}}$ of the pump parameter are determined by the expressions

$$\begin{aligned}
\Phi_{\mathrm{s}}^{\mathrm{sp}} &= \frac{1}{1+q^2s^2}\left[\frac{\exp(\alpha l) - \cos(2\pi s l/L)}{\exp(\alpha l) - 1} + \frac{q^2s^2\alpha l}{\exp(\alpha l) - 1}\right. \\
&\left.\times\frac{\sin(2\pi s l/L)}{2\pi s l/L}\right],
\end{aligned} \tag{16}$$

where $s = |k - j| = 1, 2, \dots, K - 1$; $q = 2\pi/(\alpha l)$;

$$A^{c} = \frac{A_0}{\pi}\int_0^{\pi} \Phi_{or}(\Psi - \Psi_{pump})\cos 2\Psi \, d\Psi$$
$$= A_0(1-a)\frac{2+b-2\sqrt{1+b}}{b(1+\sqrt{1+b}-a)}\cos 2\Psi_{pump},$$
$$A^{s} = \frac{A_0}{\pi}\int_0^{\pi} \Phi_{or}(\Psi - \Psi_{pump})\sin 2\Psi \, d\Psi \qquad (17)$$
$$= A_0(1-a)\frac{2+b-2\sqrt{1+b}}{b(1+\sqrt{1+b}-a)}\sin 2\Psi_{pump}.$$

To compare the results of numerical simulation with the results of the experiment on observation of the instability of stationary lasing upon intracavity frequency doubling under phase-matching conditions of the 2nd type [4], we introduced nonlinear losses responsible for nonlinear frequency conversion [12, 13] in the first two equations for the system fields (15). The parameter $\varepsilon$ is responsible for the efficiency of this process.

## 3. Results of numerical simulation and their comparison with the experimental results

The developed model can describe all the variety of peculiarities of the low-frequency dynamics of solid-state lasers pumped by linear polarised laser radiation. Figure 1 shows the dependence of the intensities of laser modes, frequencies and decrements of relaxation oscillations on the pump parameter $A$. For definiteness we assumed in calculations that $K = 14$, i.e. lasing is possible for 14 longitudinal modes in each polarisation mode. All the region of bipolarisation lasing can be divided into three regions corresponding to three regimes (Fig. 1c): monopolarisation (I), quasi-monopolarisation (II) and bipolarisation (III) regimes. This division is determined by the behaviour of all the relaxation oscillations, which reflect the low-frequency dynamics of a multimode laser. Each relaxation oscillation $\{\Omega, \delta\}$ has the frequency $\Omega$ and the damping decrement $\delta$. One can distinguish three groups in the spectrum of relaxation oscillations:

(i) In-phase relaxation oscillations $\{\Omega_1, \delta_1\}$.

(ii) Groups of low-frequency relaxation oscillations $\{\Omega_{sp}^{x}, \delta_{sp}^{x}\}$ and $\{\Omega_{sp}^{y}, \delta_{sp}^{y}\}$ caused by spatial burning out of the population inversion and characterising the out-of-phase dynamics of all longitudinal modes. The number of these oscillations is determined by the number of $x$- and $y$-polarised longitudinal modes.

(ii) Groups of relaxation oscillations $\{\Omega_2, \delta_2\}$, $\{\Omega_3, \delta_3 3\}$ and $\{\Omega_p^{xy}, \delta_p^{xy}\}$ caused by polarisation burning out of the population inversion and responsible for the out-of-phase dynamics between orthogonally polarised modes, i.e. polarisation relaxation oscillations. The number of these oscillations is determined by the number of pairs of orthogonally polarised modes with the equal longitudinal indices. These relaxation oscillations appear in region II, where the weak polarisation mode is not detected yet because of its low intensity.

The effect of induced gain anisotropy by linearly polarised pump radiation is shown in Fig. 2. The behaviour of polarisation modes is similar to their behaviour in the

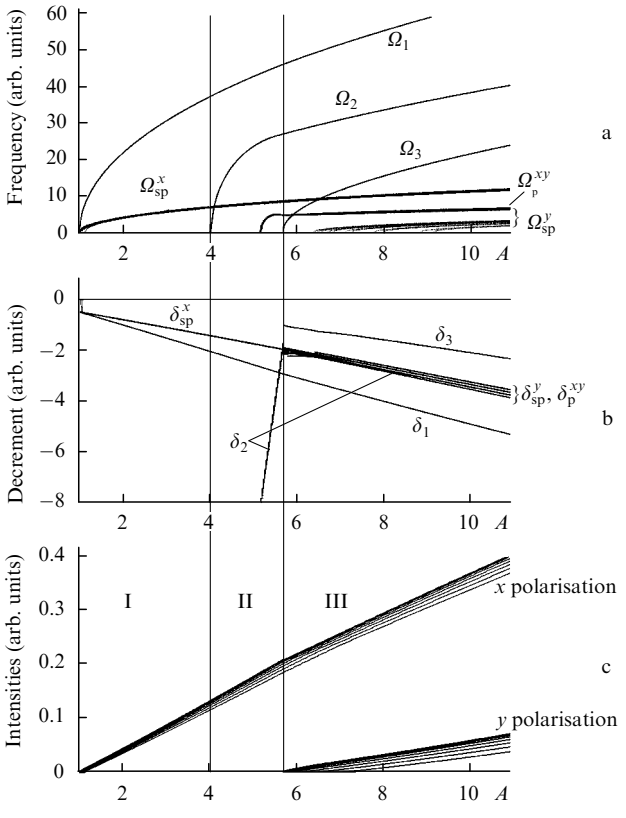


**Figure 1.** Dependence of the frequencies (a) and decrements (b) of relaxation oscillations and laser mode intensities (c) on the pump parameter $A$ for $G = 1000$, $l/L = 1$, $\alpha = 0$, $\Psi_{pump} = 0$, $\vartheta = 0$, $b = 0.5$, $a = 0$, $\delta = \Delta_0 = 0$, $\Delta = 0.01$, $\varepsilon = 0.001$.

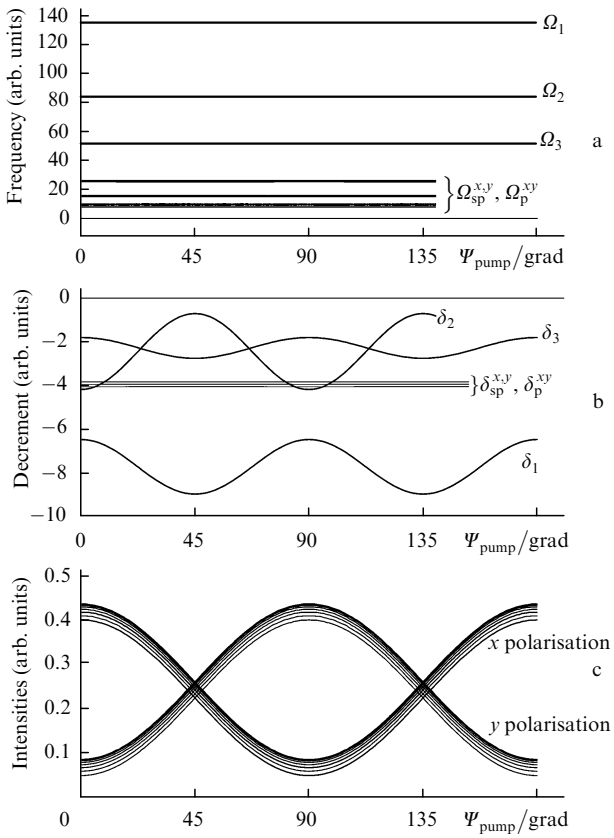


**Figure 2.** Dependence of the frequencies (a) and decrements (b) of relaxation oscillations and laser mode intensities (c) on the orientation of the pump polarisation $\Psi_{pump}$ for $A = 8$, $G = 2000$, $l/L = 1$, $\alpha = 0$, $\vartheta = 0$, $b = 0.5$, $a = 0$, $\delta = \Delta_0 = 0$, $\Delta = 0.01$, $\varepsilon = 0.001$.

case of single-mode lasing [5, 6]; the intensities of orthogonally polarised modes change out of phase with changing the orientation angle $\Psi_{\text{pump}}$ of the pump polarisation. In this case, the relaxation frequencies remain virtually constant. In the absence of intracavity nonlinear frequency conversion ($\varepsilon = 0$), all the decrements also remain almost constant. The conversion process ($\varepsilon \neq 0$) leads to the dependence of decrements $\delta_1$, $\delta_2$, $\delta_3$ on $\Psi_{\text{pump}}$ (Fig. 2b), while the other decrements remain virtually independent of the pump polarisation orientation.

A special place in the group of polarisation relaxation oscillations is taken by oscillations $\{\Omega_2, \delta_2\}$ and $\{\Omega_3, \delta_3\}$. They are responsible for out-of-phase oscillations of total intensities of orthogonally polarised modes and are present in the fluctuation spectra of total intensities of polarisation modes in the form of resonance peaks at frequencies $\Omega_2$ and $\Omega_3$ (Fig. 3). It is these oscillations that are observed in the case of single longitudinal-mode lasing together with in-phase relaxation oscillations $\{\Omega_1, \delta_1\}$.

The introduction of nonlinear intracavity losses ($\varepsilon \neq 0$) caused by nonlinear frequency doubling leads to the Hopf bifurcation at the frequency of one of the relaxation oscillations ($\{\Omega_2, \delta_2\}$ or $\{\Omega_3, \delta_3\}$) depending on the ratio of polarisation mode intensities. At a large difference in the intensities of polarisation modes, the Hopf bifurcation at frequency $\Omega_3$ is observed (Fig. 4a); the smoothing of the intensities leads to the Hopf bifurcation at frequency $\Omega_2$ (see Fig. 3 and Fig. 4c). One can see from Figs 4b and d that Hopf bifurcations at these relaxation oscillations have a different character. In the instability region in these figures (to the right of vertical dashed lines) maximum and minimum values of the polarisation mode intensities are shown. At the frequency $\Omega_3$, the Hopf bifurcation at the point $\varepsilon_{\text{HB}}^{(1)}$ has a subcritical character: self-oscillations with the finite amplitude appear above this point (Fig. 4b). One can see from Fig. 4b that the transition of the bifurcation point in the backward direction (curves with points $\Delta$ and $\nabla$) does not affect the nonstationary regime and only at the point $\varepsilon_{\text{B}}$ this regime disappears and the steady-state solution appears.

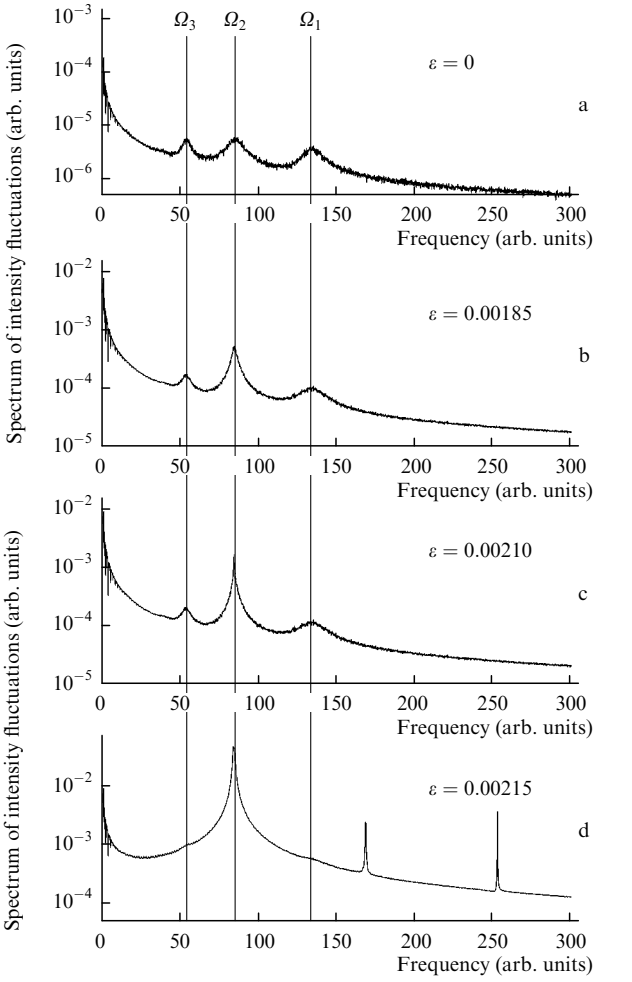


**Figure 3.** Spectra of intensity fluctuations of one of polarisation modes for different efficiencies of nonlinear frequency conversion $\varepsilon$ for $A = 8$, $G = 2000$, $\Psi_{\text{pump}} = 35^\circ$, $l/L = 1$, $\alpha = 0$, $\vartheta = 0$, $b = 0.5$, $a = 0$, $\delta = \Delta_0 = 0$, $\Delta = 0.01$.

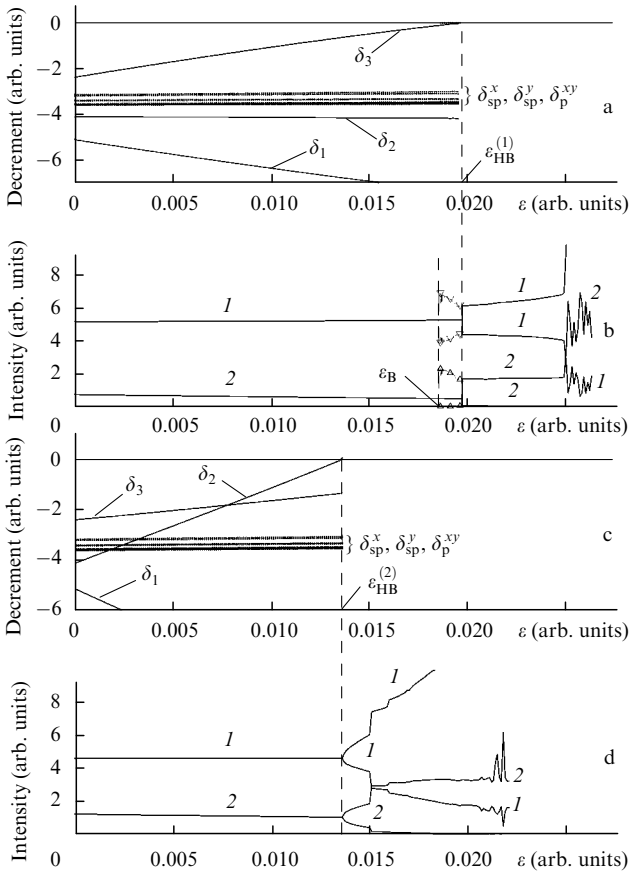


**Figure 4.** Dependence of decrements of relaxation oscillations (a, c) and intensities of $x$-polarised (*1*) and $y$-polarised (*2*) laser modes (b, d) on the nonlinear conversion efficiency $\varepsilon$ for $\Psi_{\text{pump}} = 0$ (a, b) and 20° (c, d).

Therefore, in the region $\varepsilon_{\text{B}} < \varepsilon < \varepsilon_{\text{HB}}^{(1)}$ the bistable lasing regime with the characteristic dependence of the result of the numerical simulation on initial values is realised. In another situation shown in Fig. 4d, the Hopf bifurcation of the supercritical type is realised at the point $\varepsilon_{\text{HB}}^{(2)}$ at relaxation frequency $\Omega_2$: the oscillation amplitude in the instability region increases from zero as it moves away from the bifurcation boundary.

Figure 3 demonstrates the supercritical character of Hopf bifurcations in the spectra of intensity fluctuations of an individual polarisation mode. At low efficiency of the nonlinear frequency conversion, the intensity of laser

radiation is stable and three resonance peaks at frequencies $\Omega_1$, $\Omega_2$, and $\Omega_3$ of relaxation oscillations are observed in the spectra of intensity fluctuations (Fig. 3a). Fluctuations at the frequency of one of the polarisation relaxation oscillations ($\Omega_2$) increase with increasing the efficiency of the nonlinear conversion $\varepsilon$. As a result, the resonance peak at the frequency of the polarisation relaxation oscillation becomes narrower and higher in amplitude, and above the bifurcation point this is accompanied by the appearance of many harmonics at the frequency of polarisation relaxation oscillation in the noise spectrum (Fig. 3d). This character of the instability development was also observed in the experiment (Fig. 5) [4].

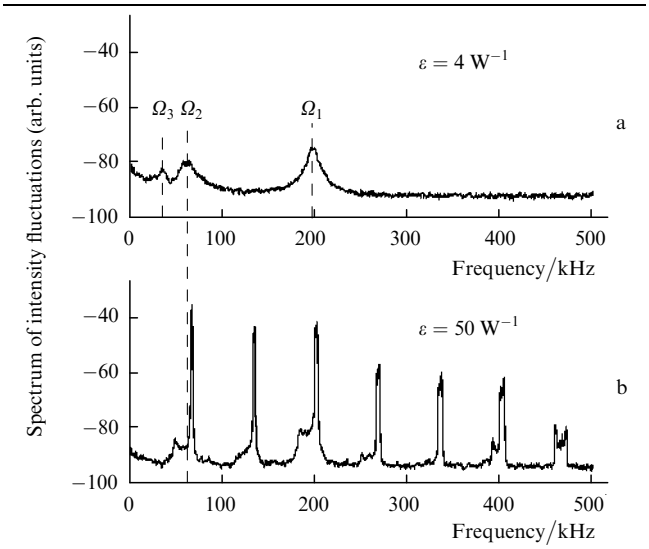


**Figure 5.** Spectra of intensity fluctuations of one of polarisation modes for a fixed pump parameter $A = 3.25$ and different efficiencies of nonlinear frequency conversion $\varepsilon$.

The developed model also allows one to explain the peculiarities in the optical spectrum of a bipolarisation laser observed in the experiment [4] (Fig. 6): along with the 'rarefaction' of the lasing spectrum, the generation of orthogonally polarised components at different longitudinal modes is also possible. The laser emits in the 1064-nm region at three longitudinal modes ($v_1$, $v_2$, $v_3$) with the same polarisation (Fig. 6a) and at one longitudinal mode ($v_4$) with orthogonal polarisation (Fig. 6b). The wavelengths of all the four oscillating modes are different; their frequency splittings are: $v_2 - v_1 = 22\Delta v_0$, $v_3 - v_1 = 36\Delta v_0$, and $v_4 - v_1 = 2\Delta v_0$, where $\Delta v_0 = c/(2L)$ is the interval between adjacent longitudinal modes of the cavity. Other longitudinal modes are suppressed due to etalon effects on different surfaces of the cavity and due to the partial filling of the cavity with the active medium [7, 14]. The radiation at the doubled frequency (Fig. 6c) exhibits three spectral components with frequencies $v_1 + v_4$, $v_2 + v_4$, and $v_3 + v_4$ obtained during frequency summing of orthogonally polarised modes.

Figure 7 shows the result of numerical simulation of multimode generation of orthogonally polarised modes at different longitudinal modes, which qualitatively agree with the experimental results (Fig. 6). It is necessary to emphasise that we observe here regime II: in each of three longitudinal modes, an almost monopolarisation lasing regime is realised because the ratio of the intensities of orthogonally polarised modes with equal longitudinal indices is of the order of

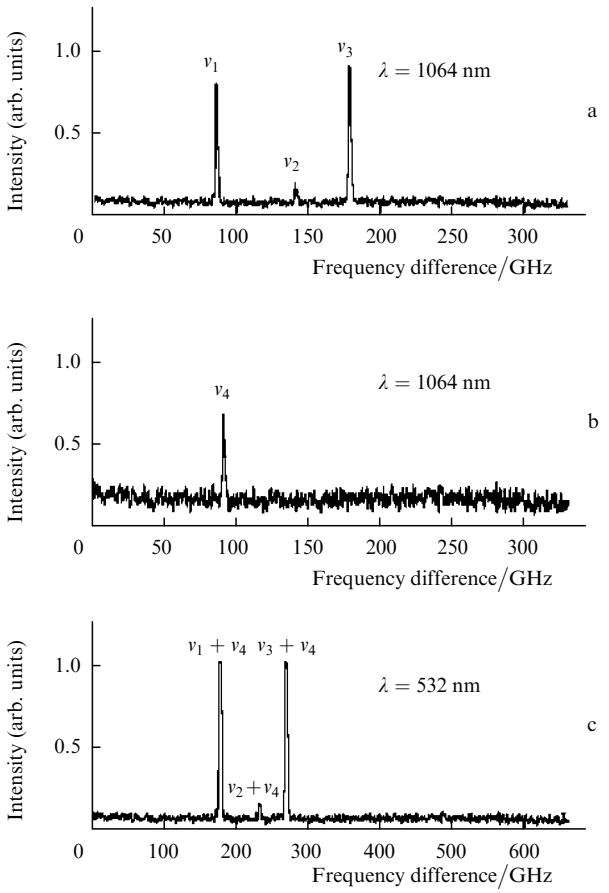


**Figure 6.** Optical radiation spectrum of a bipolarisation laser with intracavity frequency doubling: $x$-polarised (a) and $y$-polarised (b) modes and the radiation spectrum composition at the doubled frequency (c).

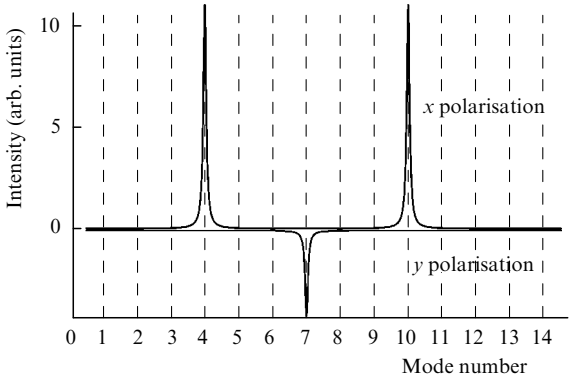


**Figure 7.** Optical spectrum of polarisation modes for $A = 8$, $\varepsilon = 0.005$, $\Psi_{\text{pump}} = 0$, $l/L = 0.1$, and $\alpha = 4$. Other parameters are as Fig. 2.

$10^{-3}$. In this equilibrium state the system has six relaxation oscillations. Three of these oscillations are shown in Fig. 3.

## 4. Conclusions

The developed model can explain all the variety of characteristic properties of the low-frequency dynamics of solid-state lasers pumped by linearly polarised laser radiation. The spectrum of relaxation oscillations contains three groups of oscillations. The special place in the group of low-frequency relaxation oscillations is occupied by polarisation relaxation oscillations $\{\Omega_2, \delta_2\}$ and $\{\Omega_3, \delta_3\}$.

They are responsible for out-of-phase oscillations of the total intensities of orthogonally polarised modes and are observed in the form of resonance peaks in the fluctuation spectrum of total intensities of polarisation modes at frequencies $\Omega_2$ and $\Omega_3$. It has been shown that introduction of nonlinear losses upon intracavity frequency doubling leads to the Hopf bifurcation at the frequency of one of relaxation oscillations – $\Omega_2$ or $\Omega_3$. The groups of low-frequency relaxation oscillations $\{\Omega_{\rm sp}^x, \delta_{\rm sp}^x\}$, $\{\Omega_{\rm sp}^y, \delta_{\rm sp}^y\}$, and $\{\Omega_{\rm p}^{xy}, \delta_{\rm p}^{xy}\}$ can be observed only in the spectrum of intensity fluctuations of separate longitudinal modes and are not observed in the fluctuation spectrum of total intensities. The theoretical investigation of the dynamics of multimode lasing of bipolarisation solid-state diode-pumped lasers with the inhomogeneous distribution of the unsaturated gain along the resonator is in qualitative agreement with the experimental studies of these lasers [1–4].

***Acknowledgements.*** This work was supported by Grant No. 7738.2006.2 of the President of the Russian Federation for Support of the Leading Scientific Schools.

## References

1. Khandokhin P.A., Khanin Ya.I., Milovsky N.D., Shirokov E.Yu., Bielawski S., Derozier D., Glorieux P. *Quantum and Semiclassical Optics*, **10**, 97 (1998).
2. Khandokhin P.A., Khanin Ya.I., Mamaev Yu.A., Milovskii N.D., Shirokov E.Yu., Bielawski S., Derozier D., Glorieux P. *Kvantovaya Elektron.*, **25** (6), 517 (1998) [*Quantum Electron.*, **28** (6), 502 (1998)].
3. Khandokhin P.A., Milovsky N.D., Mamaev Yu.A., Ovchinnikov E.A., Shirokov E.Yu. *Proc. SPIE Int. Soc. Opt. Eng.*, **3682**, 53 (1998).
4. Czeranowsky C., Baev V.M., Huber G., Khandokhin P.A., Khanin Ya.I., Koryukin I.V., Shirokov E.Yu. *Izv. Vyssh. Uchebn. Zaved., Ser. Radiofiz.*, **47** (10-11), 807 (2004).
5. Bouwmans G., Segard B., Glorieux P., Milovsky N., Khandokhin P., Shirokov E. *Izv. Vyssh. Uchebn. Zaved., Ser. Radiofiz.*, **47** (10-11), 813 (2004).
6. Ievlev I.V., Khandokhin P.A., Shirokov E.Yu. *Kvantovaya Elektron.*, **36** (3), 228 (2006) [*Quantum Electron.*, **36** (3), 228 (2006)].
7. Khandokhin P.A., Ovchinnikov E.A., Shirokov E.Yu. *Phys. Rev. A*, **61**, 053807 (2000).
8. Ovchinnikov E.A., Khandokhin P.A., Shirokov E.Yu. *Kvantovaya Elektron.*, **30** (1), 23 (2000) [*Quantum Electron.*, **30** (1), 23 (2000)].
9. Bayerer R., Heber J., Mateika D. *Zr. Phys. B*, **64**, 201 (1986).
10. Reyzer K.C., Casperson L.W. *J. Appl. Phys.*, **51**, 6075 (1980).
11. Reyzer K.C., Casperson L.W. *J. Appl. Phys.*, **51**, 6083 (1980).
12. Baer T. *J. Opt. Soc. Am. B*, **3**, 1175 (1986).
13. James G.E., Harrell II E.M., Roy R. *Phys. Rev. A*, **41**, 2778 (1990).
14. Abraham N.B., Sekaric L., Carson L.L., Seccareccia V., Khandokhin P.A., Khanin Ya.I., Koryukin I.V., Zhislina V.G. *Phys. Rev. A*, **62**, 013810 (2000).